Pergamon

0301-9322(95)00046-1

Int. J. Multiphase Flow Vol. 21, No. 6, pp. 1169–1189, 1995
Copyright © 1995 Elsevier Science Ltd
Printed in Great Britain. All rights reserved
0301-9322/95 $9.50 + 0.00

SLOW MOTIONS OF A SOLID SPHERICAL PARTICLE CLOSE TO A VISCOUS INTERFACE

K. D. DANOV[1], R. AUST[2]†, F. DURST[2] and U. LANGE[2]

[1]Laboratory of Thermodynamics and Physico-Chemical Hydrodynamics, Faculty of Chemistry, University of Sofia, J. Bourchier Ave 1, Sofia 1126, Bulgaria

[2]Lehrstuhl für Strömungsmechanik, Universität Erlangen-Nürnberg, Cauerstr. 4, D-91058 Erlangen, Germany

(Received 18 July 1994; in revised form 11 June 1995)

Abstract—In order to investigate the hydrodynamic interaction between an interface and a spherical particle and its dependence on the type of interface, it is essential to compute the drag and torque exerted on the sphere in the vicinity of the interface. In this paper, the problem of all slow elementary motions (relative translation and rotation) and stationary movement of a spherical particle next to a solid, viscous or free interface is considered. For low capillary numbers and different values of surface dilatational and shear viscosities in a curvilinear co-ordinate system of revolution with bicylindrical co-ordinates in meridian planes, the problem reduces from three to two dimensions. The model equations and boundary conditions, which contain second-order derivatives of the velocities, transform to an equivalent well-defined system of second-order partial differential equations which is solved numerically for medium and small values of the dimensionless distance to the interface. Very good agreement with the asymptotic equation for a translating sphere close to a solid interface could be achieved. The numerical results reveal in all cases the strong influence of the surface viscosity on the motion of the solid sphere. For small distances from the interface, the drag and torque coefficients change significantly depending on the surface viscosity.

Key Words: drag force, torque, spherical particle, particle–interface interaction, surface viscosity effect

1. INTRODUCTION

The description of the general rheological behaviour of colloidal materials, consisting of various phases in a multiphase flow system, requires information regarding the drag force and torque between the phases (Hunter 1987, 1989; Russel *et al.* 1989). In dilute systems the individual particle motion can be treated independently. In contrast, when the particle concentration is high, the effect of hydrodynamic interactions between the spherical particle and the interface on the drag force and torque is of considerable importance. Theoretical contributions are limited to low Reynolds numbers (mostly for creeping flows) (see review by Davis 1993; papers by Brenner 1973; Brenner & Leal 1982 and Uijttewaal *et al.* 1993 and books by Kim & Karrila 1991 and Happel & Brenner 1965), avoiding the difficulties arising from the non-linearity of the equations governing the fluid motion at higher velocities. For flow systems containing more than two particles and interfaces, the method of reflection is usually used, because it is unlikely that one will find a co-ordinate system to satisfy simultaneously all boundary conditions. A great deal of work has been done in obtaining first- and higher-order wall corrections for spheres in flows that are bounded by plane or cylindrical walls (see Happel & Brenner 1965). Faxén (1921) developed the method of reflection for a sphere translating between two parallel planes in a viscous fluid. However, this method and the solutions obtained are not valid for arbitrary distances from the wall (Hetsroni 1982).

An important step forward was achieved by Stimson & Jefferey (1926), who employed a bipolar co-ordinate system to compute the velocity field of a slow-moving fluid flowing around two equal sized spherical particles aligned in the flow direction. The status of knowledge in the field was summarized and theory and experiment were compared by Goldsmith & Mason (1967). Zhu *et al.* (1994) performed direct measurements of the drag force on two interacting solid spheres arranged in the longitudinal direction for medium Reynolds numbers. Dean & O'Neill (1963) and O'Neill (1964) showed that the force and the torque acting on a spherical particle, translating and rotating

†To whom correspondence should be addressed.

at right angles to their common diameter in a viscous fluid at an arbitrary distance in a plane parallel to the solid interface, can be accurately determined. The limiting behaviour when the sphere is almost in contact with the wall was obtained rigorously by O'Neill & Stewartson (1967), Goldman *et al.* (1967) and Cooley & O'Neill (1968). The solution is usually expressed as a series, but the coefficients of the various terms cannot be determined except as the solution of a set of difference equations. In principle it may therefore now be claimed that the problem of two spheres translating slowly through a viscous medium has been solved, apart from certain limiting situations when the series obtained either fails to converge or converges too slowly for numerical evaluation. Instead of the exact solution of the problem these authors derived an asymptotic equation for the force and torque and corrected some inaccuracies made in the previous work of Dean & O'Neill (1963) and O'Neill (1964). An important contribution towards the understanding of this problem was made by Yang & Leal (1990), who provided analytical results for the motion of a viscous Newtonian fluid drop in the presence of a plane, deformable interface in the velocity range for which inertial effects can be neglected.

Most of the publications in this field are based on the assumption that the interface is solid or free. When insoluble or soluble surfactants are present in the solution, the interface shows a viscous behaviour. Boussinesq (1913) postulated the existence of a surface viscosity, conceived as the two-dimensional equivalent of the conventional three-dimensional viscosity possessed by bulk-fluid phases. For many years, Boussinesq's solution was accepted as the basis for explaining the anomalous droplet settling velocity results available in the literature, encouraging the development of various instruments for measuring the surface viscosity and other rheological properties of fluid interfaces (Joly 1964). Boussinesq's theory was generalized to material interfaces of arbitrary curvature in the work by Sternling & Scriven (1959), together with Scriven's (1960) paper. The effects of Gibbs elasticity and surface viscosity on the drag coefficient of an emulsion droplet in adsorption-controlled Marangoni flow were considered by Levich (1962) and Edwards *et al.* (1991). They showed that, in this case, only the dilatational surface viscosity influences the drag coefficient. The effect of Gibbs elasticity is usually neglected when the concentration of insoluble surfactants is low, the diffusion of soluble surfactants is fast or the concentration of soluble surfactants is greater than the critical micelles concentration. In these cases, we can calculate the flow in the frame of Newtonian volume and surface rheology, not taking into account the equations for the surfactants mass balance.

This paper discusses the problem of determining the drag force and torque exerted on a solid sphere translating or rotating near a solid, viscous liquid or free interface for low Reynolds and capillary numbers. In the case of a viscous interface, the free surface–excess pressure tensor considers the Boussinesq (1913) and Scriven (1960) constitutive law for a Newtonian interface. It is proved in detail in section 3 that the problem for Stokes flow in a co-ordinate system of revolution with bicylindrical co-ordinates in the meridian planes can be reduced from three to two dimensions. The problem has an analytical solution only for free and solid interfaces. For viscous interfaces, the boundary conditions contain second-order derivatives of the velocity, hence no analytical solution exists. Stokes equations and the boundary conditions are transformed to an equivalent well-defined system of second-order partial differential equations with known boundary conditions using the "two vorticities–one velocity" formulation which is convenient for numerical computations. In order to illustrate the global interaction between a spherical particle and a viscous interface and its dependence on the distance from the interface the drag force and the torque coefficients, in addition to the velocity and pressure distributions, are obtained and described in section 4 for all elementary motions which are components of the stationary velocity and pressure distribution. The numerical results reveal a strong dependence of the motion (rotation and translation) of the solid sphere on the surface viscosity numbers when it is close to the surface.

2. BASIC EQUATIONS AND BOUNDARY CONDITIONS

We consider the stationary motion of a solid; spherical particle in a viscous; incompressible fluid next to a plane solid, viscous liquid or free interface. On one side of the interface the liquid is assumed to be unbounded and on the other side a gas or a solid wall is assumed. When remaining

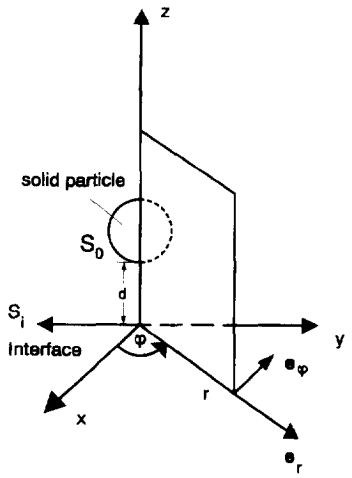

Figure 1. Geometry of the system.

in the frame of low Reynolds number hydrodynamics, the pressure p and the local fluid velocity $\mathbf{v}$ obey Stokes' equations for creeping motion:

$$\nabla \cdot \mathbf{v} = 0, \quad \eta \nabla^2 \mathbf{v} = \nabla p \qquad [1]$$

where η is the dynamic viscosity and ∇ is the volume gradient. Owing to the linearity of the equations governing the flow, each particle motion can be presented as a superposition of a translational motion along and a rotational motion around an axis parallel to the plane and a translation along and a rotation around the axis perpendicular to the plane. The influence of the surface viscosity on the film mobility and drainage rate was investigated by Zapryanov *et al.* (1983) and the problem of a solid, spherical particle rotating around the axis perpendicular to the solid wall was solved by O'Neill & Ranger (1979). In this paper we consider the other elementary motions of a solid spherical particle with radius a and surface S_0 performing either translational motion parallel to the Oy axis or rotation with the angular velocity parallel to the Ox axis (see figure 1). The boundary condition on the solid sphere is

$$\mathbf{v} = \mathbf{v}_0 \quad \text{at} \quad S_0 \qquad [2]$$

where $\mathbf{v}_0$ is the velocity of the sphere. The other boundary condition on the interface S_i depends on the type of interface. For a solid interface the velocity on it is zero and for a free interface the friction is zero (see Yang & Leal 1990). For a Newtonian viscous liquid interface S_i (see Scriven 1960 and Edwards *et al.* 1991) we consider the Boussinesq–Scriven constitutive law and define the surface-excess stress tensor $\mathbf{S}$ in the following form (compare, for example, [4.2-15] to [4.2-18] in Edwards *et al.* 1991)

$$\mathbf{S} = \sigma \mathbf{I}_s + (\eta_d - \eta_{sh})(\nabla_s \cdot \mathbf{v}_s)\mathbf{I}_s + \eta_{sh}[(\nabla_s \mathbf{v}_s) \cdot \mathbf{I}_s + \mathbf{I}_s \cdot (\nabla_s \mathbf{v}_s)^T] \qquad [3]$$

where σ is the thermodynamic interfacial tension, which in our case is considered to be constant, η_{sh} and η_d are the interfacial shear and dilatational viscosities at a given point of the interface respectively, $\mathbf{I}_s$ is the unit surface idemfactor, $\mathbf{v}_s$ is the surface velocity and ∇_s is the surface gradient (see appendices 4.A and 4.B in Edwards *et al.* 1991 for the definition of the surface operators). Equation [3] is the two-dimensional analogue of the comparable expressions for the bulk-phase pressure tensor $\mathbf{P}$:

$$\mathbf{P} = -p\mathbf{I} + \eta[\nabla \mathbf{v} + (\nabla \mathbf{v})^T] \qquad [4]$$

In [3] and [4], $(\nabla_s \mathbf{v}_s)^T$ and $(\nabla \mathbf{v})^T$ are the transposes of the tensors $(\nabla_s \mathbf{v}_s)$ and $(\nabla \mathbf{v})$, respectively. In all practical circumstances the surface-excess mass density is small compared with the bulk-phase mass density and the equation for the interfacial momenum transport reduces to the balance of the forces acting on the material interface (see, for example, [4.2-20], [4.2-20a] and [4.2-20b] in Edwards *et al.* 1991):

$$\nabla_s \cdot \mathbf{S} = \mathbf{n}_s \cdot \langle \mathbf{P} \rangle \qquad [5]$$

where $\mathbf{n}_s$ is the unit normal to the viscous liquid interface and $\langle \mathbf{P} \rangle$ is the jump of the volume stress tensor $\mathbf{P}$. In addition we must also take into account the usual kinematic boundary condition.

The resultant force $\mathbf{F}$, due to the stress, exerted by the surrounding fluid on the surface of the solid spherical particle S_0 and the torque $\mathbf{M}$ experienced by the body surface are (see Happel & Brenner 1965)

$$\mathbf{F} = \int_{S_0} \mathbf{P}\cdot\mathbf{n}\, dS_0, \quad \mathbf{M} = \int_{S_0} (\mathbf{r}_0 \times \mathbf{P})\cdot\mathbf{n}\, dS_0 \qquad [6]$$

where $\mathbf{r}_0$ is the position vector of a point relative to an origin at the centre of the sphere (see figure 1) and $\mathbf{n}$ is the vector of the running unit normal to the particle surface S_0. The problem under consideration at small Reynolds numbers is linear for a solid interface. For free and viscous interfaces the boundary conditions [3]–[5] depend on the capillary number $C = \eta V_*/\sigma$, where V_* is the characteristic velocity of the relative particle motion for the translational motion and ωa for the sphere rotating with angular velocity ω. Usually this number is small for many practical systems. Therefore, it seems to be justified that from now on we can consider the case where $C \to 0$ with the assumption that the interface at $z = 0$ remains planar. In this case, the boundary conditions can be linearized. Then the interactions between a particle and an interface are additive and the stationary particle motion in the liquid flow can be presented as a superposition of translational and rotational elementary motions. Hence the hydrodynamic drag force and torque of a moving particle are counterbalanced by those connected with the external forces:

$$\mathbf{F}_m + \mathbf{F}_r + \mathbf{F}_b = 0, \quad \mathbf{M}_m + \mathbf{M}_r = 0 \qquad [7]$$

where $\mathbf{F}_m$, $\mathbf{F}_r$ and $\mathbf{M}_m$, $\mathbf{M}_r$ are, respectively, the drag force and the torque of translation and rotation and $\mathbf{F}_b$ is the external force (for example, buoyancy force parallel to the non-disturbed surface).

3. MATHEMATICAL MODEL OF THE PROBLEM

The system of [1] and boundary conditions [2]–[5] are difficult to compute directly numerically using the velocity–pressure formulation or the vorticity formulation. The difficulties are connected with the specific form of the equations and were discussed by Fletcher (1991a, b). Here we shall transform the problem into the equivalent well-defined system of second-order partial differential equations with known boundary conditions in a rectangular region, which is convenient for numerical investigations.

We denote by $Oxyz$ a system of Cartesian co-ordinates, φ is a meridian angle, any plane for which φ is constant is a meridian plane and r and z are, respectively, radial and vertical co-ordinates in a cylindrical co-ordinate system $Or\varphi z$ (see figure 1). The region $z < 0$ is either a solid wall or air whereas for $z > 0$ a liquid phase is assumed. All dimensionless co-ordinates are introduced by scaling with the particle radius a. Let x_1 and x_2 be bicylindrical co-ordinates in the meridian planes (see figure 2) connected with the Cartesian co-ordinates with the following expressions:

$$x = \frac{b \sin x_2 \cos \varphi}{\cosh x_1 - \cos x_2}, \quad y = \frac{b \sin x_2 \sin \varphi}{\cosh x_1 - \cos x_2}, \quad z = -\frac{b \sinh x_1}{\cosh x_1 - \cos x_2} \qquad [8]$$

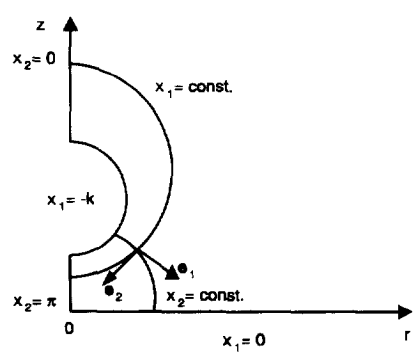

Figure 2. Bicylindrical co-ordinates x_1 and x_2 in the plane Orz. The circle of radius 1, corresponding to the line $x_1 = -k$, represents the projection of the particle surface.

where the bicylindrical parameter b and the regions of the co-ordinates are

$$b^2 = (1+d)^2 - 1, \quad -k \leqslant x_1 \leqslant 0, \quad 0 \leqslant x_2 \leqslant \pi \tag{9}$$

In this co-ordinate system the lines $x_1 = \text{constant}$ and $x_2 = \text{constant}$ are circumferences shown in figure 2, the projection of the particle surface on the meridian plane is a co-ordinate line

$$x_1 = -k, \quad k = \ln(1+d+b), \quad h = \frac{1}{b}(\cosh x_1 - \cos x_2), \tag{10}$$

h is the metric coefficient and d is the minimum dimensionless distance between the sphere and the interface.

After eliminating the pressure from the Stokes equations [1], one obtains a general equation for the vorticity vector $\mathbf{w}$

$$\mathbf{w} = \tfrac{1}{2}\nabla \times \mathbf{v}, \quad \nabla \times \nabla \times \mathbf{w} = \mathbf{0} \tag{11}$$

All cases considered above have linearized boundary conditions for elementary motions such that the solution of the equations contains only one mode of a Fourier expansion. Therefore, the dimensionless velocity and vorticity components in the given co-ordinate system can be presented in the following general form

$$\mathbf{v} = V_*(v_1 \sin\varphi, v_2 \sin\varphi, v_\varphi \cos\varphi), \quad \mathbf{w} = \frac{V_*}{ab}(w_1 \cos\varphi, w_2 \cos\varphi, w_\varphi \sin\varphi) \tag{12}$$

The components of the velocity in the meridian plane are connected with the components of the vorticity in this plane as follows:

$$v_1 = h\frac{\partial}{\partial x_1}(rv_\varphi) + \frac{2r}{b}w_2, \quad v_2 = h\frac{\partial}{\partial x_2}(rv_\varphi) - \frac{2r}{b}w_1 \tag{13}$$

The boundary conditions [3]–[5] contain second-order derivatives of the velocity which make the computation of the problem more complicated. We use the two vorticities w_1 and w_2—one velocity v_φ formulation of the problem. With the abbreviations

$$A_1 = -\frac{\sinh x_1}{\cosh x_1 - \cos x_2}, \quad A_2 = \frac{\cosh x_1 \cos x_2 - 1}{\sin x_2(\cosh x_1 - \cos x_2)}, \quad A_3 = \frac{\sin x_2}{\cosh x_1 - \cos x_2},$$

we can write from [1], [12] and [13] the equation of continuity in the following form

$$\frac{\partial^2 v_\varphi}{\partial x_1^2} + \frac{\partial^2 v_\varphi}{\partial x_2^2} + 3A_1\frac{\partial v_\varphi}{\partial x_1} + 3A_2\frac{\partial v_\varphi}{\partial x_2} + \frac{2}{bh}\frac{\partial w_2}{\partial x_1} - \frac{2}{bh}\frac{\partial w_1}{\partial x_2} + \frac{6A_1}{bh}w_2 - \frac{2}{bh}(2A_2 - A_3)w_1 = 0 \tag{14}$$

After substituting [12] into [11], we can derive a system of second-order partial differential equations for the components of the vorticity vector. It is not necessary to compute the component perpendicular to the meridian plane, because it is not included in [13]. Hence,

$$\frac{\partial^2 w_1}{\partial x_1^2} + \frac{\partial^2 w_1}{\partial x_2^2} + 3A_1\frac{\partial w_1}{\partial x_1} + A_2\frac{\partial w_1}{\partial x_2} - 2A_3\frac{\partial w_2}{\partial x_1} + (A_1^2 - A_2^2 - A_3^2)w_1 - 3A_1A_3w_2 = 0,$$

$$\frac{\partial^2 w_2}{\partial x_1^2} + \frac{\partial^2 w_2}{\partial x_2^2} + A_1\frac{\partial w_2}{\partial x_1} + 3A_2\frac{\partial w_2}{\partial x_2} + (1 - 3A_1^2)w_2 + 2(A_2 + A_3)\frac{\partial w_1}{\partial x_1} + 2A_1\frac{\partial w_1}{\partial x_2} + A_1(A_3 + 4A_2)w_1 = 0. \tag{15}$$

Let us transform the boundary conditions of the problem for the defined functions. For the case of a solid spherical particle translating with constant relative velocity in the Oy direction, the boundary conditions [2] for the dimensionless meridian velocity component and [2] and [13] for the dimensionless vorticity components at the surface S_0 read

$$v_\varphi = 1, \quad w_1 = 0, \quad \frac{2}{bh}w_2 + \frac{\partial v_\varphi}{\partial x_1} = 0 \quad \text{at} \quad x_1 = -k \tag{16}$$

For a sphere rotating with constant angular velocity parallel to the Ox axis, similar boundary conditions can be written in the following form

$$v_\varphi = 1 + d - z, \quad w_1 = b^2 h A_1 A_3, \quad \frac{2}{bh} w_2 + \frac{\partial v_\varphi}{\partial x_1} = b A_2 A_3 \quad \text{at} \quad x_1 = -k \tag{17}$$

At infinity the values of the two vorticities w_1 and w_2 and the velocity v_φ go to zero. For all types of interfaces (solid, free and viscous) the linearized kinematic boundary condition (the normal component of the velocity is equal to zero) for our computation yields

$$\frac{2}{bh} w_2 + \frac{\partial v_\varphi}{\partial x_1} = 0 \quad \text{at} \quad x_1 = 0. \tag{18}$$

Considering the problem when the sphere is close to the solid interface, the velocity on it and the first component of the vorticity are zero. For a free interface the friction is neglected and the normal derivatives of the meridian component of the velocity and the first component of the vorticity are zero on it. For a viscous interface, the tangential components of the linearized stress boundary conditions [3]–[5] using the definitions in [12] and [13] and [14] can be reduced to the following system of second-order partial differential equations for the velocity component v_φ and vorticity component w_1 at the interface $x_1 = 0$:

$$\frac{\partial v_\varphi}{\partial x_1} = (K + E)h\left[\frac{\partial^2 v_\varphi}{\partial x_2^2} + (A_3 + 3A_2)\frac{\partial v_\varphi}{\partial x_2}\right] - \frac{2K}{b}\frac{\partial w_1}{\partial x_2} - 4(K + E)\frac{A_2}{b} w_1,$$

$$\frac{\partial w_1}{\partial x_1} = Eh\left[\frac{\partial^2 w_1}{\partial x_2^2} + (A_2 + A_3)\frac{\partial w_1}{\partial x_2} - A_2^2 w_1\right] + A_3 w_2 \tag{19}$$

where $K = \eta_d/\eta a$ and $E = \eta_{sh}/\eta a$ are the dilatational and the shear surface viscosity number, respectively. When the surface viscosity numbers are zero, one obtains from [19] the well-known conditions for the free interface. However, the usual definition of the surface viscosity numbers cannot give the correct description of the hydrodynamic interaction close to the liquid interface, because in [19] the surface viscosity numbers are divided by the bicylindrical parameter b, and this parameter is several orders of magnitude smaller than 1 when the dimensionless distance to the interface is very small. From [14] and [15] one can derive the asymptotic behaviour of the meridian component of the velocity and the components of vorticity on the axis of revolution:

$$\frac{\partial v_\varphi}{\partial x_2} = 0, \quad w_1 = 0, \quad \frac{\partial w_2}{\partial x_2} = 0 \quad \text{at} \quad x_2 = 0 \quad \text{and} \quad x_2 = \pi \tag{20}$$

Using the definitions [12] and [13], one can compute the physical components of the velocity. Finally, the pressure is derived from [1] in the meridian plane using [12] and [13] for the velocity

$$p = \frac{\eta V_*}{a} q \sin\varphi, \quad q = 2rh^2\left[\frac{\partial}{\partial x_2}\left(\frac{w_1}{h}\right) - \frac{\partial}{\partial x_1}\left(\frac{w_2}{h}\right)\right] \tag{21}$$

After substituting [12] and [21] into [4] and [6], we could prove that in our case only the y component of the drag force and the x component of the torque exerted by the surrounding fluid were non-zero. The general forms of these are

$$F_y = f\pi\eta a V_*, \quad M_x = m\pi\eta a^2 V_* \tag{22}$$

where the dimensionless drag coefficient f and the dimensionless torque coefficient m are represented by the following expressions:

$$f = f_0 + \int_0^\pi \left\{-r\frac{\partial r}{\partial x_1} q + r\left[1 - \frac{\partial}{\partial x_2}\left(rh^2\frac{\partial r}{\partial x_2}\right)\right]\frac{\partial v_\varphi}{\partial x_1} - \frac{2hr}{b}\frac{\partial r}{\partial x_2}\frac{\partial r w_1}{\partial x_1}\right\} dx_2,$$

$$m = m_0 + \int_0^\pi \left(\frac{2r}{b}\frac{\partial r w_1}{\partial x_1} + r^2\frac{\partial h}{\partial x_2}\frac{\partial v_\varphi}{\partial x_1}\right) dx_2 \tag{23}$$

In [23] the additional coefficients f_0 and m_0 are zero for a translating sphere. For a rotating sphere they have an analytical form:

$$f_0 = \int_0^{\pi} \frac{b^2 \sin^3 x_2 (\cosh k \cos x_2 - 1)}{(\cosh k - \cos x_2)^5} (4 \sinh^2 k + \cosh k \cos x_2 - 1)\, dx_2,$$

$$m_0 = \int_0^{\pi} \frac{b^2 \sin^3 x_2}{(\cosh k - \cos x_2)^4} (1 - 2 \sinh^2 k - \cosh k \cos x_2)\, dx_2 \qquad [24]$$

The normal component of the linearized stress boundary conditions [3]–[5] in the cases of free and viscous interfaces gives the equation for the first Fourier mode deviation of the shape S_1. The disturbances of the surface shape are proportional to the capillary number C and in our case the effect of the deformation of the interface is of second order. In fact, if the sphere is very close to the interface, e.g. about 0.1 μm or less, then the Van der Waals, electrostatic, steric, etc., interactions are more important than hydrodynamic interactions (Danov *et al.* 1993) and the motion of the spherical particle depends on them, the deformation of the interface cannot be neglected and the problem is non-linear and very difficult to solve numerically.

The numerical investigation of the problem considered here is also very complex because boundary condition [19] contains the second derivative of the meridian component of the velocity and of the first component of the vorticity. However, different numerical methods for solving [14] and [15] with the boundary conditions [16]–[18] and [20] can be used (Brebbia 1978; Fletcher 1984, 1991a, b). We used the modified alternating direction implicit method proposed by Danov *et al.* (1994) for a similar problem, which gives the possibility of computing with second-order implicit time and space variable interpolations.

4. NUMERICAL RESULTS AND DISCUSSIONS

4.1. Velocity and pressure distribution

In order to illustrate the influence of the hydrodynamic interactions between a sphere and an interface on the global velocity and pressure distribution and their dependence on the type interface (solid, viscous or free) and on the dimensionless distance from the interface, we computed the flow field for a translating and a rotating sphere. In figure 3 the numerical results obtained for the velocity field in the vicinity of a spherical particle in the plane $x = 0$ are shown. The sphere translates with a velocity of 1 at distance 1 from the interface, which is located at $z = 0$. One can see that changing the viscosity of the interface from low viscous [figure 3(a)] to solid [figure 3(b)], not only changes the boundary layer close to the interface but also affects the whole flow field around the sphere. The corresponding pressure distributions are plotted in figure 4(a) and (b). The isobars illustrate the anti-symmetric pressure distribution in the plane $x = 0$ (see [21]). The pressure maximum develops just below the equatorial plane ($z = 2$) when the interface is of low viscosity. With increasing surface viscosity numbers it moves in the direction of the interface and the magnitude of the pressure gradient and the absolute values of the pressure increase considerably. By comparing figure 4(a) and (b) one can also see that the pressure acting on the interface rises significantly with increasing interface viscosity. In the region above the sphere, the pressure gradients are less pronounced and, close to the z-axis, the pressure and the velocity distribution are comparable to the Stokes solution. In order to illustrate the influence of the distance of the sphere from the surface, the pressure distribution on the viscous interface ($z = 0$) is plotted in figure 5(a) (low viscous interface) and (b) (highly viscous interface) for a distance of 0.01.

The velocity distribution in the plane $x = 0$ for a sphere rotating near the low viscous or solid interface is shown in figure 6(a) and (b), respectively. In both cases, the disturbance of the fluid through the rotating movement is restricted to the area close to the sphere and the influence of the solid interface on the motion is less significant. The flow field above the sphere close to the z-axis is almost identical with Kirchhoff's solution. The corresponding isobars are shown in figure 7(a) and (b). The behaviour of the pressure distribution is similar to that in the previous case, but the absolute values of the pressure are about half. Also, the pressure distribution on the interface for small distances is different. The numerical results obtained for a low viscous interface

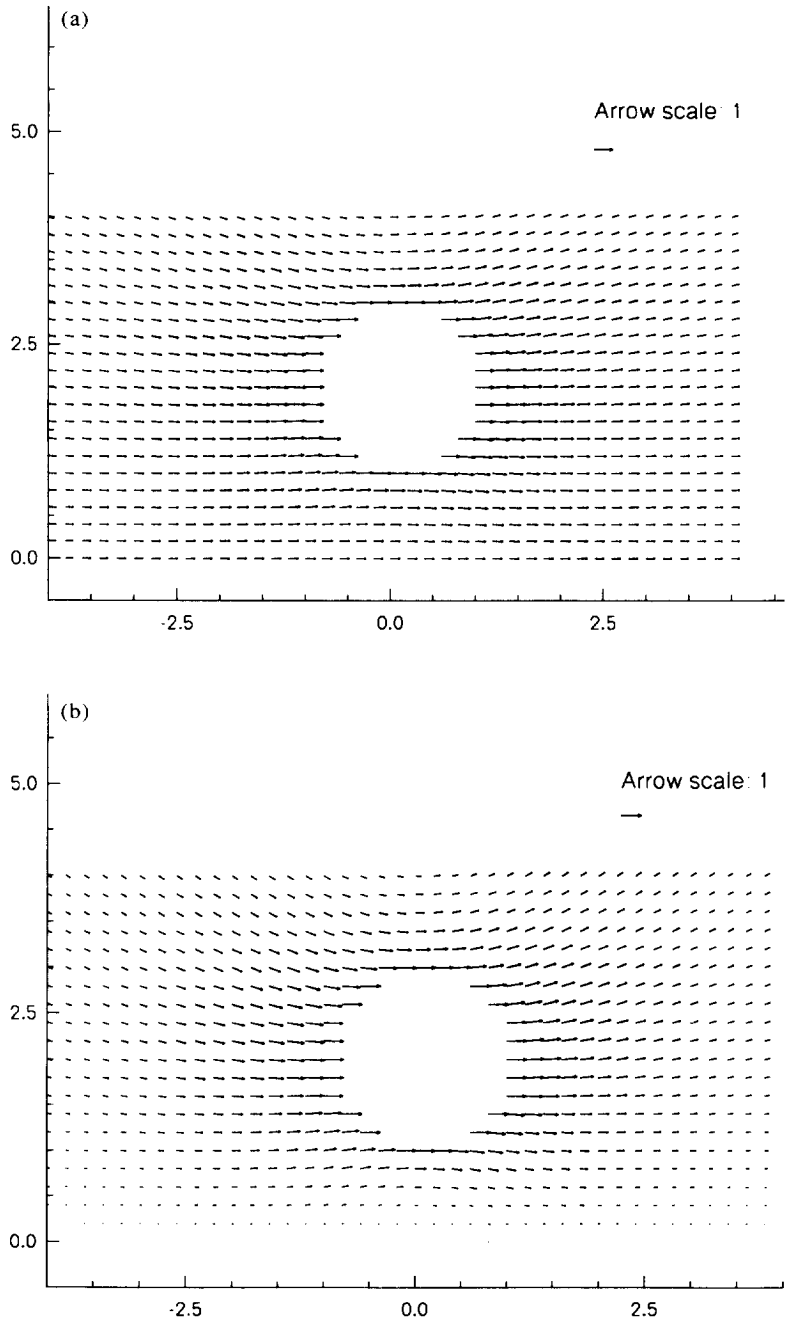

Figure 3. Velocity field for a spherical particle translating in the plane $x = 0$ for dimensionless distance 1 in the cases of: (a) low viscous interface and (b) solid interface.

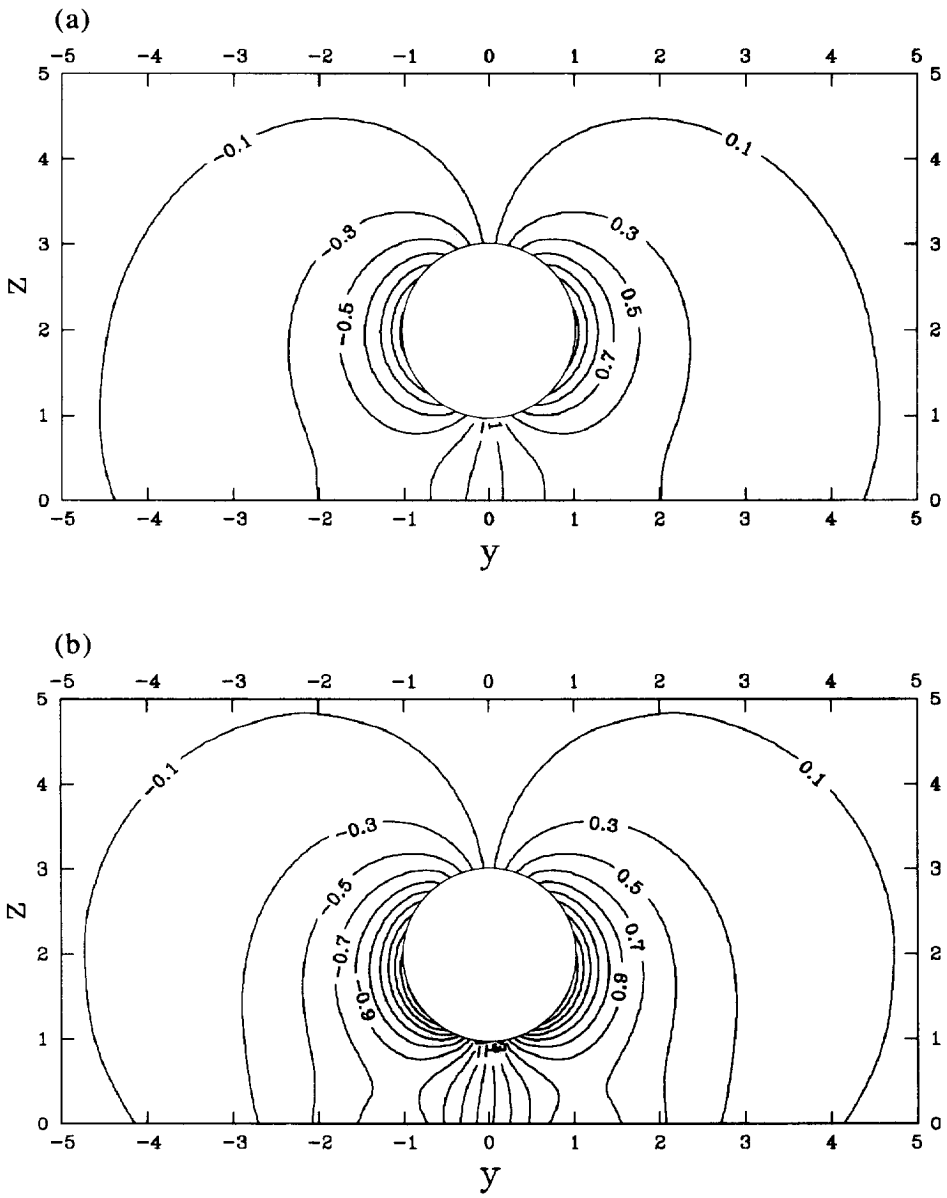

Figure 4. Pressure distribution for a spherical particle translating in the plane $x = 0$ for dimensionless distance 1 in the cases of: (a) low viscous interface and (b) solid interface.

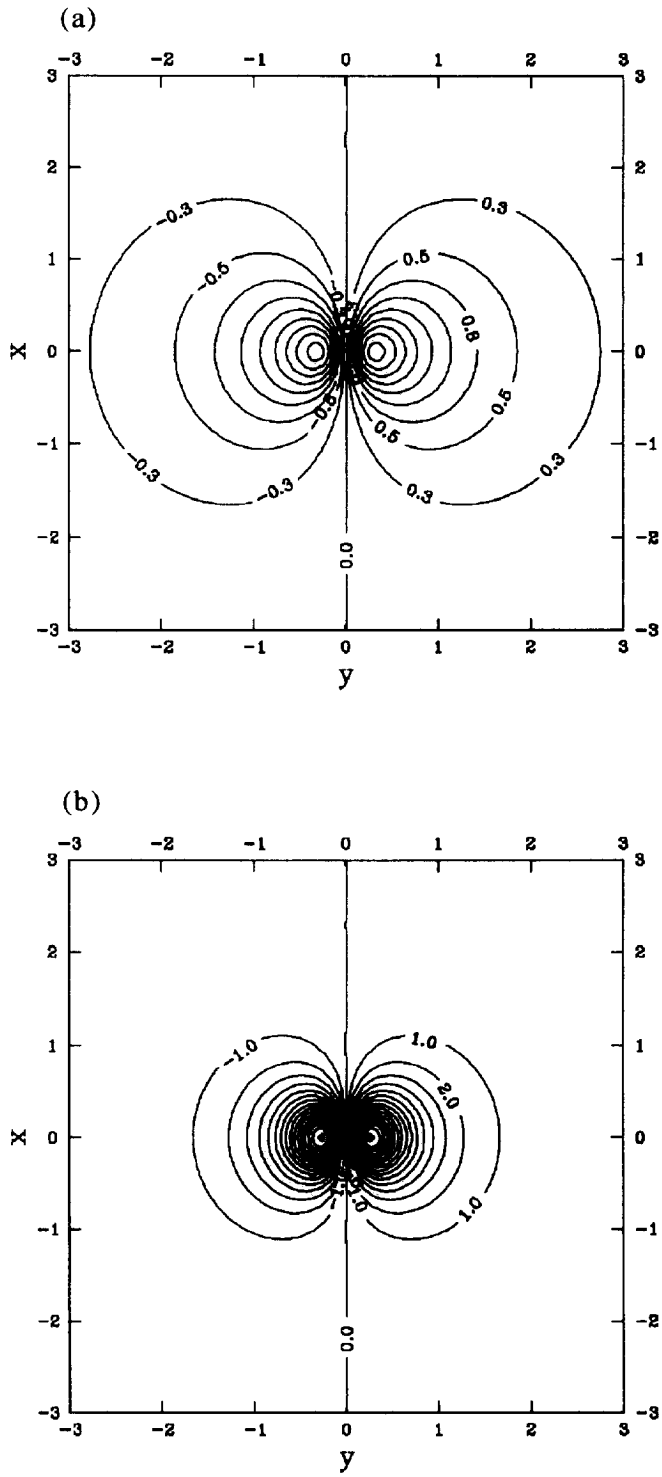

Figure 5. Pressure distribution on the interface for a sphere translating close to it in the cases of: (a) low viscous interface and (b) high viscous interface.

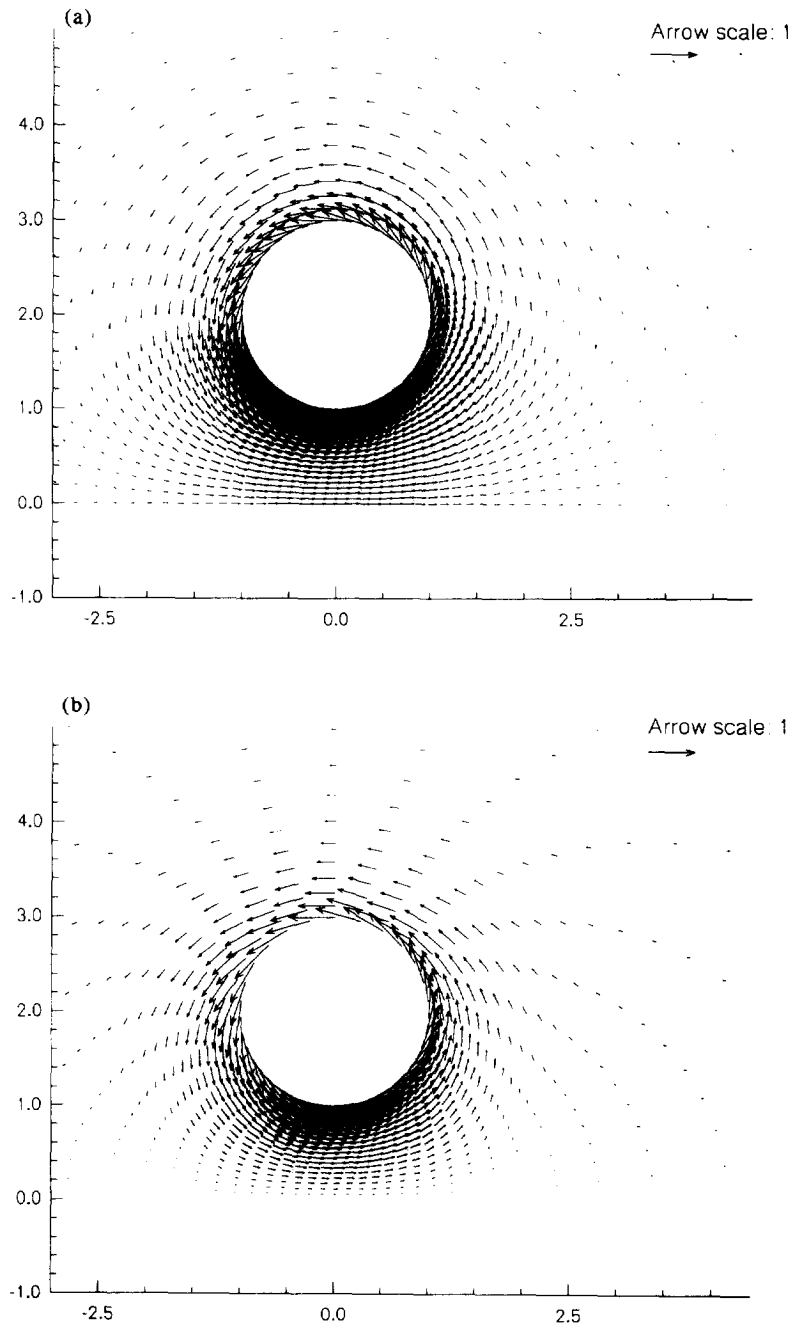

Figure 6. Velocity field for a spherical particle rotating in the plane $x = 0$ for dimensionless distance 1 in the cases of: (a) low viscous interface and (b) solid interface.

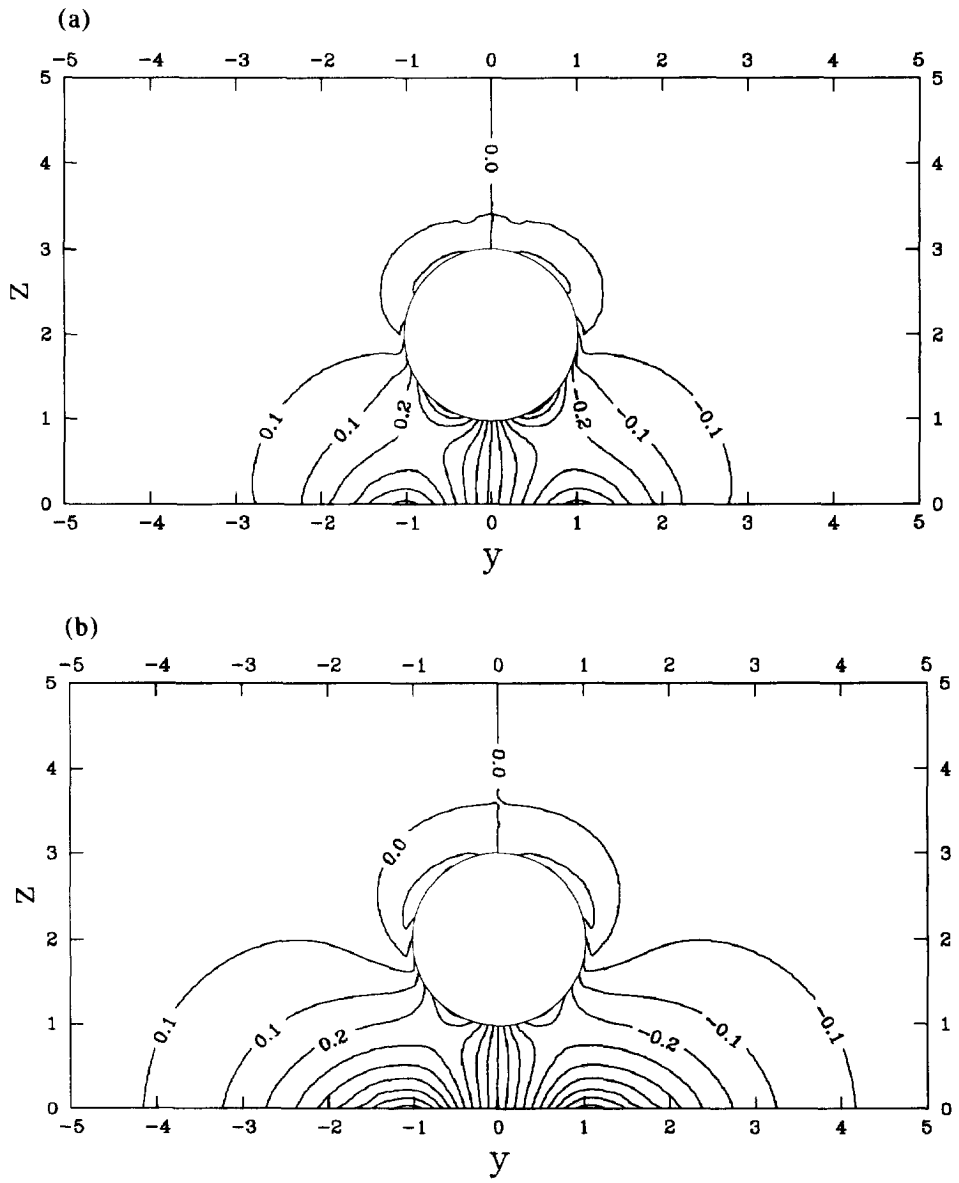

Figure 7. Pressure distribution for a spherical particle rotating the plane $x = 0$ for dimensionless distance 1 in the cases of: (a) low viscous interface and (b) solid interface.

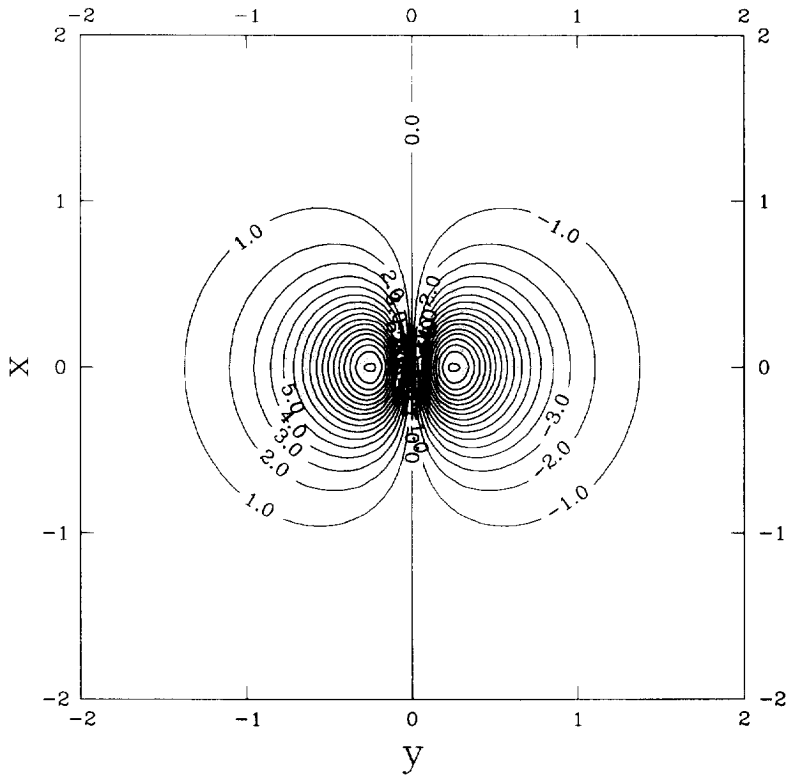

Figure 8. Pressure distribution on the low viscous interface for a sphere rotating close to it.

and a distance of 0.01 between the sphere and the interface are illustrated in figure 8. Here the influence of the surface viscosity is not so important. For example, if the surface viscosity number increases from 1 to 100, the maximum dimensionless pressure increases from 17.3 to 17.8.

Clearly, the pressure induced by the moving sphere will lead to a deformation of the interface, which is plotted in figure 9(a) and (b) for the translating and the rotating sphere close to a highly viscous interface, respectively. In both cases the absolute value of the disturbance is proportional to the capillary number. In these plots the deformation is enlarged, however, in order to give a better impression of the shape of the deformed surface.

4.2. Drag and torque coefficients

For a detailed investigation of the influence of the type of interface on the hydrodynamic interaction and the drag and torque coefficients as defined by [23] and [24] we performed two different types of analysis: (a) for solid, free and viscous interfaces corresponding to three typical values of the surface viscosity number we computed the dependence of the drag and torque coefficients on the distance from the interface for distances from 0.001 to 1; (b) for three values of the distance 0.01, 0.1 and 1.0 we varied the surface viscosity numbers from 0.0 (the case of a free interface) to 100.0 (the case of a highly viscous interface). The numerical results are illustrated in figures 10–13.

The dependences of the drag and torque coefficient on the distance from the interface for a translating sphere are shown in figure 10(a) and (b), respectively. Curve (a) represents our numerical results for a solid interface. Curve (b) represents the asymptotic equations of O'Neill & Stewartson (1967):

$$f = -6\left[\left(\frac{8}{15}+\frac{16}{375}d\right)\ln\left(\frac{2}{d}\right)+0.58461+O(d)\right],$$

$$m = -8\left[\left(\frac{1}{10}+\frac{43}{250}d\right)\ln\left(\frac{2}{d}\right)-0.26227+O(d)\right] \qquad [25]$$

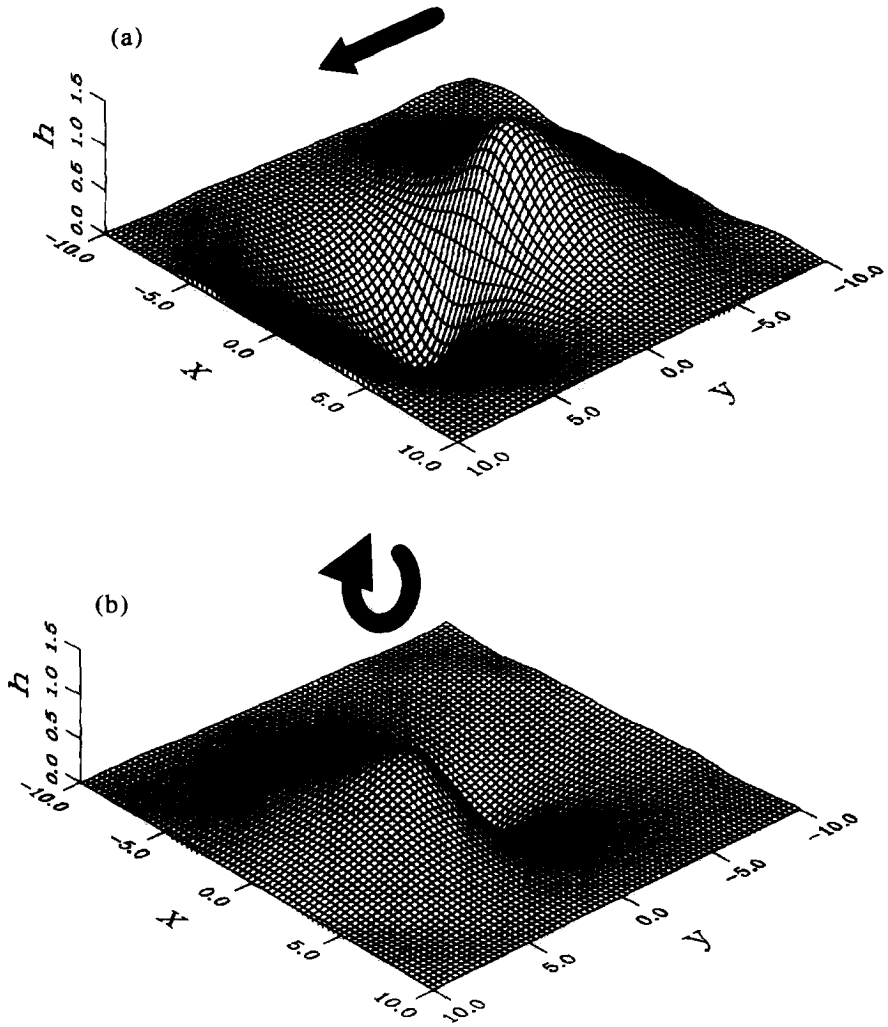

Figure 9. Typical disturbances of the viscous interface contours: (a) translating sphere and (b) rotating sphere.

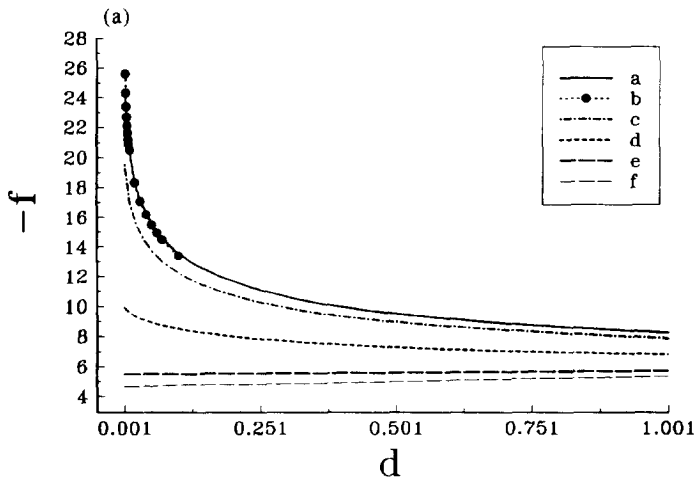

Figure 10(a). Dependence of the drag coefficient on the distance from the interface for a rotating sphere: curves (a) solid interface, (b) the asymptotic equation of O'Neill & Stewartson (1967), (c) $K = E = 100$, (d) $K = E = 10$, (e) $K = E = 1$ and (f) free interface.

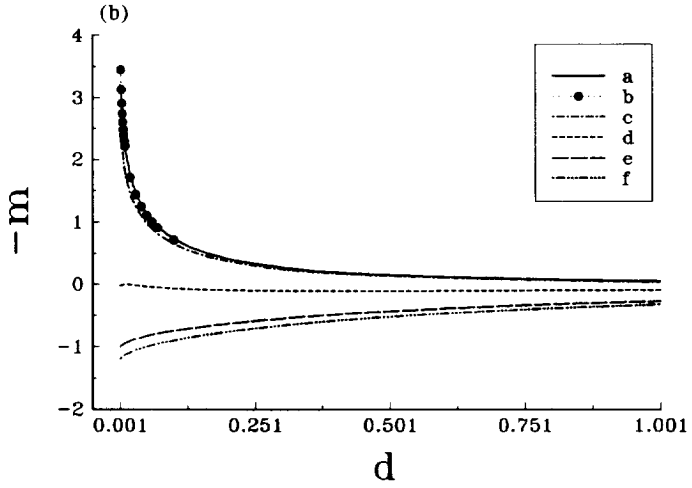

Figure 10(b). Dependence of the torque coefficient on the distance from the interface for a translating sphere: curves (a) solid interface, (b) the asymptotic equation of O'Neill & Stewartson (1967), (c) $K = E = 100$, (d) $K = E = 100$, (e) $K = E = 1$ and (f) free interface.

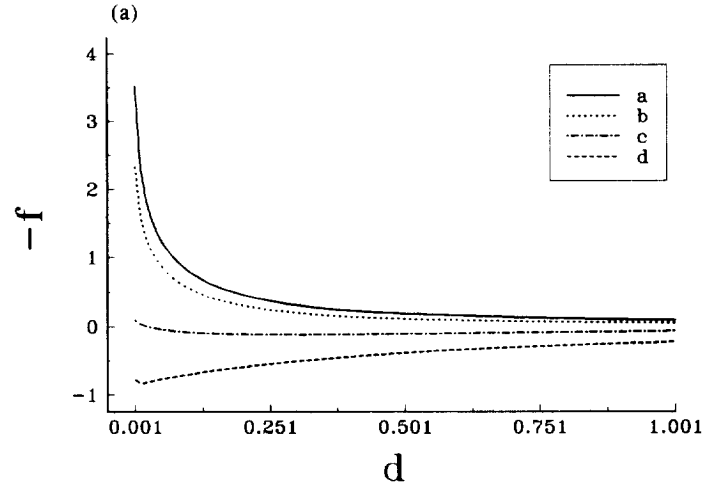

Figure 11(a). Dependence of the drag coefficient on the distance from the interface in the case of a rotating sphere: curves (a) solid interface, (b) $K = E = 100$, (c) $K = E = 10$ and (d) $K = E = 1$.

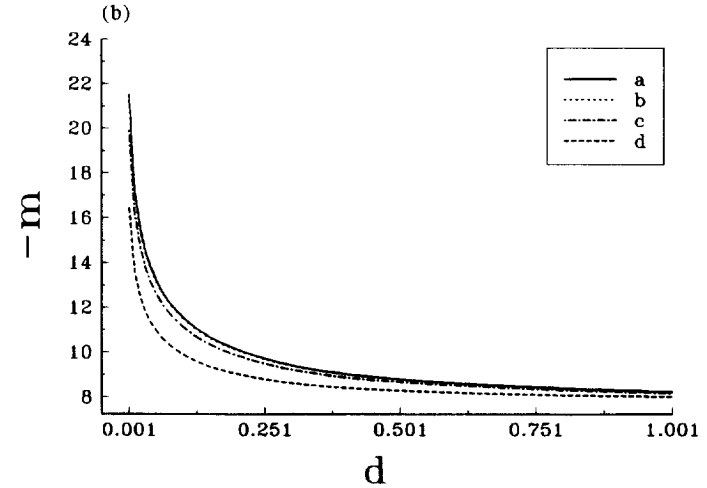

Figure 11(b). Dependence of the torque coefficient on the distance from the interface in the case of a rotating sphere: curves (a) solid interface, (b) $K = E = 100$, (c) $K = E = 10$ and (d) $K = E = 1$.

Curves (c), (d) and (e) are computed for surface viscosity numbers of 100.0, 10.0 and 1.0 and curve (f) is for a free interface. The agreement with the asymptotic equations of O'Neill & Stewartson (1967) is excellent. The influence of the surface viscosity and hence the presence of surfactants is most significant when the sphere is very close to the interface. For solid and highly viscous interfaces, the interactions increase very strongly in this area. The drag coefficient changes more than 6-fold for dimensionless distances from 1.0 to 0.001. For a medium viscous interface the drag increases very slowly in this area and, in principle, the sphere starts to interact with them only when very close to them, from $d \approx 0.01$. In contrast, for low viscous and free interfaces [curves (e) and (f)] the drag coefficient remains almost constant or drops when the sphere approaches the surface. These significant differences in the basic behaviour of the curves can best be understood by looking at the pressure plots in figure 4(a) and (b). Apparently, varying the surface viscosity numbers not only leads to changes in the interface properties but also influences the whole flow field up to a certain distance from the surface. At higher viscosity numbers very steep velocity and pressure gradients build up in the vicinity of the sphere and it is this boundary layer which is responsible for the steep increase in the drag coefficient. However, as the absolute value of f exceeds the value of Stokes solution ($f = 6$) even at larger distances, a global influence of the surface viscosity is noticeable. For low surface viscosities, almost no boundary layer develops around the sphere and

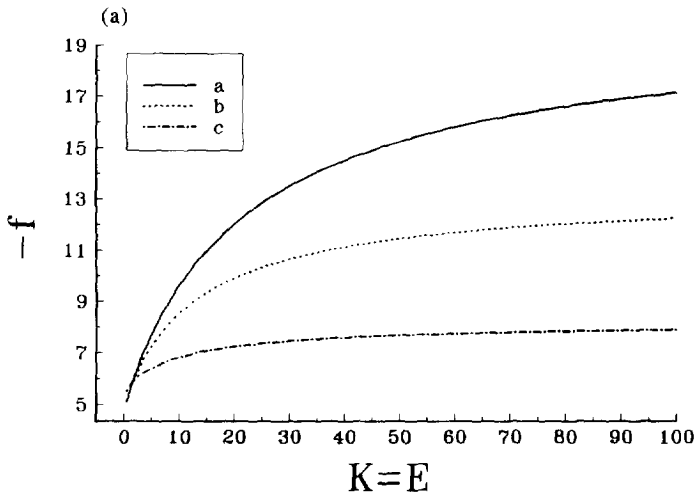

Figure 12(a). Influence of the surface viscosity numbers on the drag coefficient in the case of a translating sphere: curves (a) $d = 0.01$, (b) $d = 0.1$ and (c) $d = 1.0$.

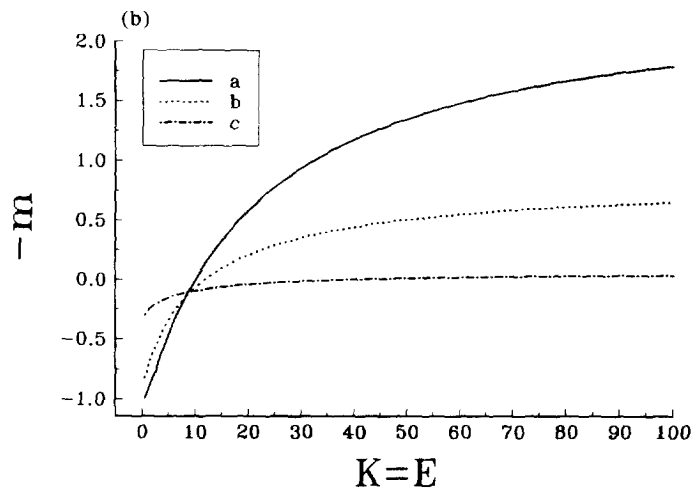

Figure 12(b). Influence of the surface viscosity numbers on the torque coefficient in the case of a translating sphere: curves (a) $d = 0.01$, (b) $d = 0.1$ and (c) $d = 1.0$.

hence, no particular effects can be perceived when the sphere approaches the interface. However, as the liquid film between the sphere and the interface becomes thinner, less fluid is moved by the sphere and therefore the absolute value of the drag coefficient drops below the Stokes solution. For $K = E = 1$ [curve (e)] the two effects balance each other at $f \approx 6$.

The torque coefficient is plotted in figure 10(b) for the same range of surface viscosity numbers as in figure 10(a). Again, the agreement with the asymptotic solution of O'Neill & Stewartson (1967) is excellent. One can see that the sign of the torque coefficient is different for low and high viscosity numbers, respectively. This means that a sphere would tend to rotate in different directions depending on the magnitude of the surface viscosity. Obviously the friction with the bulk is larger than the friction with the interface for low surface viscosities, and vice versa.

The drag and torque coefficients for a rotating sphere are presented in figure 11(a) and (b) for (a) a solid surface, (b) $K = E = 100$, (c) $K = E = 10$ and (d) $K = E = 1$. From figure 11(a), it can be deduced that the rotating sphere would tend to move in one direction for high viscosity numbers [curves (a) and (b)] and in the opposite direction for low surface viscosity numbers. At a viscosity number of about 10 [curve (c)], the rotating sphere would not translate through the liquid. When the spherical particle approaches a highly viscous interface, the force acting on it increases by an order of magnitude in the range under consideration. The torque coefficient, plotted in figure 11(b), starts

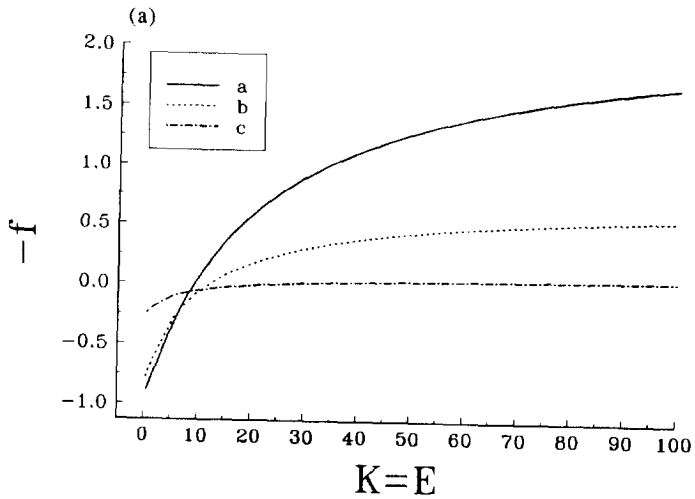

Figure 13(a). Influence of the surface viscosity numbers on the drag coefficient in the case of a rotating sphere: curves (a) $d = 0.01$, (b) $d = 0.1$ and (c) $d = 1.0$.

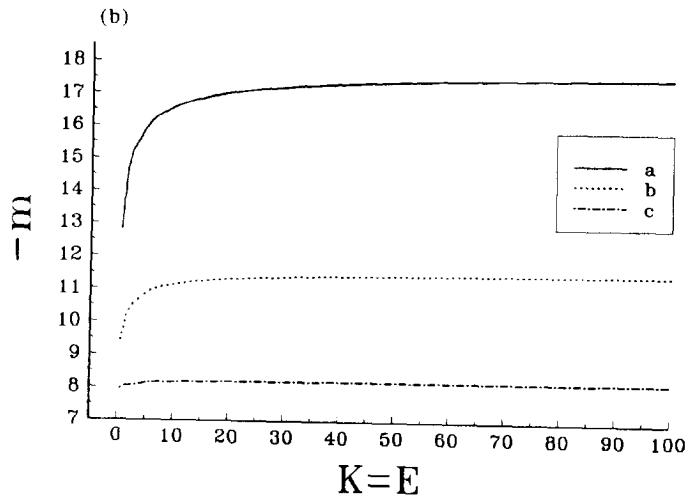

Figure 13(b). Influence of the surface viscosity numbers on the torque coefficient in the case of a rotating sphere: curves (a) $d = 0.01$, (b) $d = 0.1$ and (c) $d = 1.0$.

from an absolute value of about 8 which corresponds to Kirchhoff's solution, and reaches very high values when the sphere rotates close to the wall. This effect is almost as pronounced for moderate as for high surface viscosity numbers.

In figure 12(a), the drag coefficient of a sphere translating parallel to the interface is plotted as a function of the surface viscosity numbers for three different distances from the interface, (a) 0.01, (b) 0.1 and (c) 1.0. From this plot, a critical surface viscosity number of about 2 can be identified from the intersection point of the three curves. At this point the drag coefficient has the value of the Stokes solution. On increasing the surface viscosity number above this critical value, the influence of the surface viscosity prevails. In contrast, for lower values, the drag reduction due to the vanishing amout of liquid between the sphere and the interface is the governing effect. On considering the behaviour of the torque coefficient [figure 12(b)], the effect is similar. However, the curves do not intersect at $m = 0$ as one would expect from the previous plot.

For a rotating sphere, the critical viscosity number at which the nature of the governing effect changes [see figure 13(a) and (b)] changes from the drag to the torque coefficient.

One has to remember that for elementary motions, which are considered here, the translating sphere is not allowed to rotate and the rotating sphere is not allowed to translate. Hence, the torque coefficient of the translating sphere and the drag coefficient of the rotating sphere are secondary effects. This explains why the point or range of intersection is not exactly at $m = 0$ and $f = 0$, respectively.

4.3. *Stationary motion*

In the presence of an external force acting parallel to the y-axis, the stationary motion of the spherical particle is a superposition of the two elementary motions: the translational motion with a drag coefficient f_m, a torque coefficient m_m and a stationary translational velocity V_{st} and a rotation with the angular velocity parallel to the x-axis with a drag coefficient f_r, a torque coefficient m_r and a stationary angular velocity ω_{st}. Then [7] can be written in the following form:

$$f_m V_{st} + f_r a\omega_{st} = -6V_{Stokes}, \quad m_m V_{st} + m_r a\omega_{st} = 0 \qquad [26]$$

From [26] we computed the stationary values of the translational and angular velocity of the sphere close to the different types of interfaces. These velocities are normalized by the Stokes velocity for the unbounded fluid and they are shown in figure 14(a) and (b), respectively, as a function of the dimensionless distance for different types of surfaces: (a) solid, (b) $K = E = 100$, (c) $K = E = 10$ and (d) $K = E = 1$. The stationary velocity of the sphere is less than the Stokes value for solid and highly viscous interfaces and it decreases very significantly when the distance from the interface decreases. The motion for $d = 0.001$ is about four times slower than that for $d = 1.0$. The effect

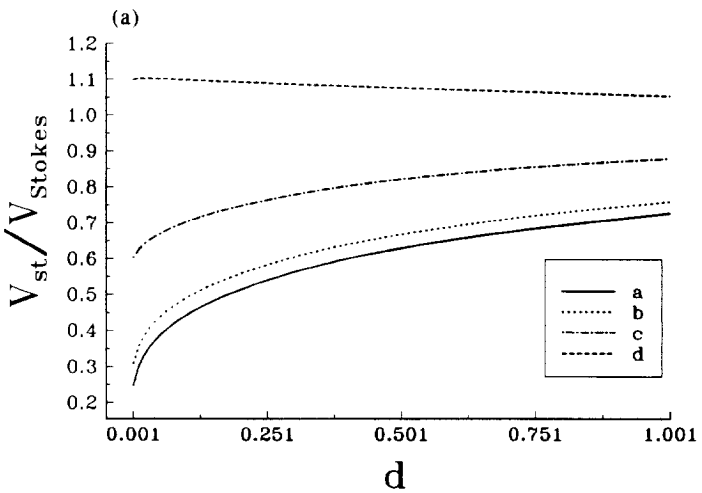

Figure 14(a). Influence of the surface viscosity numbers and distance from the interface on the stationary translation velocity V_{st} in the presence of the buoyancy force: curves (a) solid interface, (b) $K = E = 100$, (c) $K = E = 10$ and (d) $K = E = 1$.

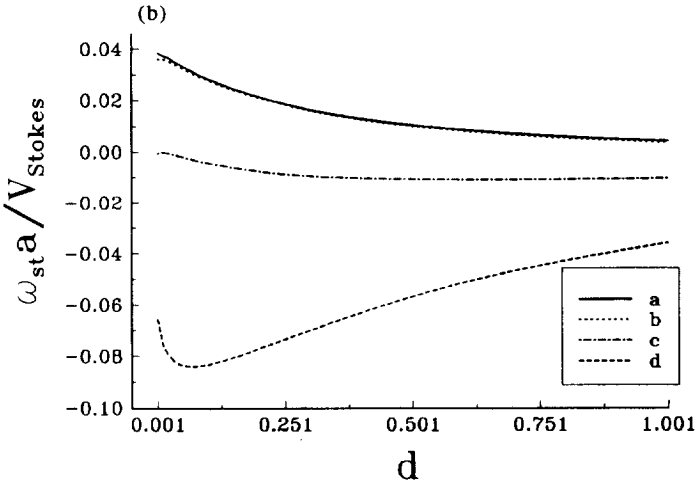

Figure 14(b). Influence of the surface viscosity numbers and distance from the interface on the stationary angular velocity ω_{st} in the presence of the buoyancy force: curves (a) solid interface, (b) $K = E = 100$, (c) $K = E = 10$ and (d) $K = E = 1$.

is the opposite for low viscous and free interfaces. In these cases, the sphere moves faster near the boundary than in the unlimited fluid. The stationary rotation of a sphere close to the solid or highly viscous interface is in the positive direction [see figure 14(b), curves (a) and (b)]. For medium surface viscosity numbers, the sphere does not rotate [curve (c)] and for low viscous interfaces the friction with the outer fluid is stronger than the interaction with the boundaries and the direction of the rotation has the opposite sign [curve (d)].

5. CONCLUSIONS

The model presented here for computing drag force and torque makes it possible to investigate the influence of the surface viscosity on the motion of a solid spherical particle close to a viscous interface. It can be used for small Reynolds and capillary numbers for solid, free and Newtonian viscous interfaces obeying the Boussinesq–Scriven constitutive law. Our computations revealed that the presence of surfactants can increase the drag exerted on a sphere translating close to a viscous interface to a value up to four times higher than the Stokes solution. Likewise, the torque acting on a rotating sphere can be considerably larger than for the case of an interface which is free of surfactants. The increase in drag and torque is partly counterbalanced by the fact that the friction reduces the more, the less liquid is present between the sphere and the interface. A critical value of about 2 for the surface viscosity numbers could be identified at which the nature of the governing effect changes. The increase in drag due to the modified surface conditions can slow the motion of a sphere considerably in comparison with a sphere moving in the vicinity of an interface which is free of surfactants. Depending on the properties of the interface, the spherical particle can rotate in either direction or not rotate at all, when travelling close to the surface, owing to the above-mentioned counteracting effects.

Acknowledgements—We are indebted to Professor I. B. Ivanov for most helpful discussions. We are also grateful for the advice provided by Dr H. Raszillier. This work was supported financially by the Volkswagen-Stiftung. The authors gratefully acknowledge this support of their collaborative research.

REFERENCES

Boussinesq, M. J. 1913 Sur l'éxistance d'une viscosité superficielle, dans la mince couche de transition separant un liquide d'une autre fluide contigue. *Ann. Chim. Phys.* **29**, 349–357.

Brebbia, C. A. 1978 *The Boundary Element Method for Engineers*. Pentech Press, London.

Brenner, H. 1973 Rheology of a dilute suspension of axisymmetric Brownian particles. *Int. J. Multiphase Flow* **1,** 195–341.

Brenner, H. & Leal, G. L. 1982 Conservation and constitutive equations for adsorbed species undergoing surface diffusion and convection at a fluid–fluid interface. *J. Colloid Interface Sci.* **88,** 136–184.

Cooley, M. D. A. & O'Neill, M. E. 1968 On the slow rotation of a sphere about a diameter parallel to a nearby plane wall. *J. Inst. Math. Appl.* **4,** 163–173.

Danov, K. D., Aust, R., Durst, F. & Lange, U. 1995 Influence of the surface viscosity on the drag and torque coefficients of a solid particle in a thin liquid layer. *Chem. Engng Sci.* **50,** 263–277.

Danov, K. D., Petsev, D. N., Denkov, N. D. & Borwankar, R. 1993 Pair interaction energy between deformable drops and bubbles. *J. Chem. Phys.* **99,** 7179–7189.

Davis, R. H. 1993 Microhydrodynamics of particulate suspensions. *Adv. Colloid Interface Sci.* **43,** 17–50.

Dean, W. R. & O'Neill, M. E. 1963 A slow motion of viscous liquid caused by a slowly rotating solid sphere. *Mathematika* **10,** 13–24.

Edwards, D. A., Brenner, H. & Wasan, D. T. 1991 *Interfacial Transport Processes and Rheology.* Butterworth–Heinemann, Boston, MA.

Faxén, H. 1921 Dissertation, Uppsala University.

Fletcher, C. A. J. 1984 *Computational Galerkin Methods.* Springer, New York.

Fletcher, C. A. J. 1991a *Computational Techniques for Fluid Dynamics Volume I.* Springer, New York.

Fletcher, C. A. J. 1991b *Computational Techniques for Fluid Dynamics Volume II.* Springer, New York.

Goldman, A. J., Cox, R. G. & Brenner, H. 1967 Slow viscous motion of a sphere parallel to a plane wall. *Chem. Engng Sci.* **22,** 637–651.

Goldsmith, H. L. & Mason, S. G. 1967 The microrheology of dispersions. In *Rheology: Theory and Applications Volume 4* (Edited by Eirich, F. R.), pp. 85–250. Academic Press, New York.

Happel, J. & Brenner, H. 1965 *Low Reynolds Number Hydrodynamics with Special Applications to Particulate Media.* Prentice–Hall, New York.

Hetsroni, G. 1982 *Handbook of Multiphase System* (Edited by Hetsroni, G.). Hemisphere, Washington, DC.

Hunter, R. J. 1987 *Foundation of Colloid Science Volume I.* Clarendon Press, Oxford.

Hunter, R. J. 1989 *Foundation of Colloid Science Volume II.* Clarendon Press, Oxford.

Joly, M. 1964 Surface viscosity. In *Recent Progress in Surface Science Volume I* (Edited by Danielli, J. F., Pankhurst, K. G. A. & Riddiford, A. C.), pp. 1–50. Academic Press, New York.

Kim, S. & Karrila, S. J. 1991 *Microhydrodynamics: Principles and Selected Applications.* Butterworth–Heinemann, Boston, MA.

Levich, V. G. 1962 *Physicochemical Hydrodynamics.* Prentice–Hall, Englewood Cliffs, NJ.

O'Neill, M. E. 1964 A slow motion of viscous liquid caused by a slowly moving solid sphere. *Mathematika* **11,** 67–74.

O'Neill, M. E. & Ranger, K. B. 1979 Rotation of a sphere in two phase flow. *Int. J. Multiphase Flow* **5,** 143–148.

O'Neill, M. E. & Stewartson, K. 1967 On the slow motion of a sphere parallel to a nearby plane wall. *J. Fluid Mech.* **27,** 705–724.

Russel, W. B., Saville, D. A. & Schowalter, W. R. 1989 *Colloid Dispersions.* Cambridge University Press, Cambridge, MA.

Scriven, L. E. 1960 Dynamics of a fluid interface. *Chem. Engng Sci.* **12,** 98–108.

Sternling, C. V. & Scriven, L. E. 1959 Interfacial turbulence: hydrodynamic instability and the Marangoni effect. *AIChE Jl* **5,** 514–523.

Stimson, M. & Jeffery, G. B. 1926 The motion of two spheres in a viscous fluid. *Proc. R. Soc. Lond. A* **111,** 110–116.

Uijttewaal, W. S. J., Nijhof, E.-J. & Heethaar, R. M. 1993 Droplet migration, deformation, and orientation in the presence of a plane wall: a numerical study compared with analytical theories. *Phys. Fluids A* **5,** 819–825.

Yang, S.-M. & Leal, L. G. 1990 Motion of a fluid drop near a deformable interface. *Int. J. Multiphase Flow* **16,** 597–616.

Zapryanov, Z., Malhotra, A. K., Aderangi, N. & Wasan, D. T. 1983 Emulsion stability: an analysis of the effects of bulk and interfacial properties on film mobility and drainage rate. *Int. J. Multiphase Flow* **9,** 105–129.

Zhu, C., Liang, S.-C. & Fan, L.-S. 1994 Particle wake effects on the drag force of an interactive particle. *Int. J. Multiphase Flow* **20,** 117–129.